Real-time full-field photoacoustic imaging using an ultrasonic camera

Oluwaseyi Balogun
Brad Regez
Northwestern University
Department of Mechanical Engineering
2137 North Tech Drive
Evanston, Illinois 60208

Hao F. Zhang
University of Wisconsin-Milwaukee
Department of Electrical Engineering and Computer Science
P.O. Box 784
Milwaukee, Wisconsin 53201

Sridhar Krishnaswamy
Northwestern University
Department of Mechanical Engineering
2137 North Tech Drive
Evanston, Illinois 60208

Abstract. A photoacoustic imaging system that incorporates a commercial ultrasonic camera for real-time imaging of two-dimensional (2-D) projection planes in tissue at video rate (30 Hz) is presented. The system uses a Q-switched frequency-doubled Nd:YAG pulsed laser for photoacoustic generation. The ultrasonic camera consists of a 2-D 12×12 mm CCD chip with 120×120 piezoelectric sensing elements used for detecting the photoacoustic pressure distribution radiated from the target. An ultrasonic lens system is placed in front of the chip to collect the incoming photoacoustic waves, providing the ability for focusing and imaging at different depths. Compared with other existing photoacoustic imaging techniques, the camera-based system is attractive because it is relatively inexpensive and compact, and it can be tailored for real-time clinical imaging applications. Experimental results detailing the real-time photoacoustic imaging of rubber strings and buried absorbing targets in chicken breast tissue are presented, and the spatial resolution of the system is quantified. [DOI: 10.1117/1.3420079]

Keywords: photoacoustic imaging; real-time imaging; ultrasonic camera.

Paper 09325SSRR received Aug. 1, 2009; revised manuscript received Mar. 10, 2010; accepted for publication Mar. 16, 2010; published online Apr. 28, 2010.

1 Introduction

Noninvasive imaging of the anatomy and functions of the subcutaneous microvasculature using systems with high precision and real-time capability remains a formidable challenge. The challenge stems from unavailability of imaging systems with the capability to meet the requirements for high sensitivity, high spatial resolution, sufficient penetration depth, high image contrast, fast imaging speed, system portability, and low cost.

Photoacoustic (PA) imaging is an excellent candidate for vascular imaging that potentially meets all of the preceding requirements. PA techniques rely on the generation of acoustic waves following the local absorption of a short-pulse laser illumination that results in local heating and transient thermoelastic expansion.[1–14] The amplitude and temporal characteristics of the generated acoustic waves are related to the optical, thermal, and elastic properties of the medium and the characteristics of the laser source. Thus, PA techniques used in biological media allow for local mapping of the optical absorption contrast sources through the measurement of the laser-generated acoustic waves.

Owing to the significantly lower acoustic scattering than optical scattering in biological tissue, PA techniques permit imaging at longer penetration depths than is achievable with purely optical techniques. The spatial resolution of PA techniques depends on the bandwidth of the laser-generated acoustic waves, and in the limit of high signal-to-noise ratio (SNR) and aberration-free acoustic wave detection, the spatial resolution can approach the acoustic diffraction limit. PA techniques have been shown to provide sufficient resolution for *in vivo* imaging of vascular structures[4–7] and tumor angiogenesis,[8] and for monitoring the concentration of oxygen,[9] and glucose[10] in blood vessels.

At present, the majority of the PA imaging techniques use either focused single-element transducers[11] or one-dimensional (1-D) linear array transducers.[12–14] In the former, a focused transducer is mechanically scanned from one point to the next along the tissue surface, and at each point, a PA A-scan signal along the axis of the transducer is acquired. By combining multiple A-scan signals obtained sequentially during scanning, cross-sectional PA images of the transducers focal region in the tissue are obtained.

Alternatively, linear array transducers allow for the acquisition of multiple A-scan signals without the need for mechanical scanning. The array transducer signals are acquired sequentially using a parallel multichannel system. The measured data are in turn processed offline using computer-based synthetic aperture reconstruction algorithms in order to obtain cross-sectional PA images. PA imaging of tissue vasculature using transducer array systems with parallel multichannel data acquisition systems have been reported.[12–14]

While these applications demonstrate the strength of PA imaging in tissue, existing techniques are still susceptible to motion artifacts associated with respiration and patient movements since the images are not acquired in a single-shot. Furthermore, PA imaging using linear array transducers also provides a limited view of the interrogated tissue. A two-

Address all correspondence to: Sridhar Krishnaswamy, Northwestern University, Department of Mechanical Engineering, 2137 North Tech Drive, Evanston, Illinois 60208, Tel: 847–491–4006; Fax: 847–491–5227; E-mail: s-krishnaswamy@northwestern.edu

1083-3668/2010/15(2)/021318/6/$25.00 © 2010 SPIE

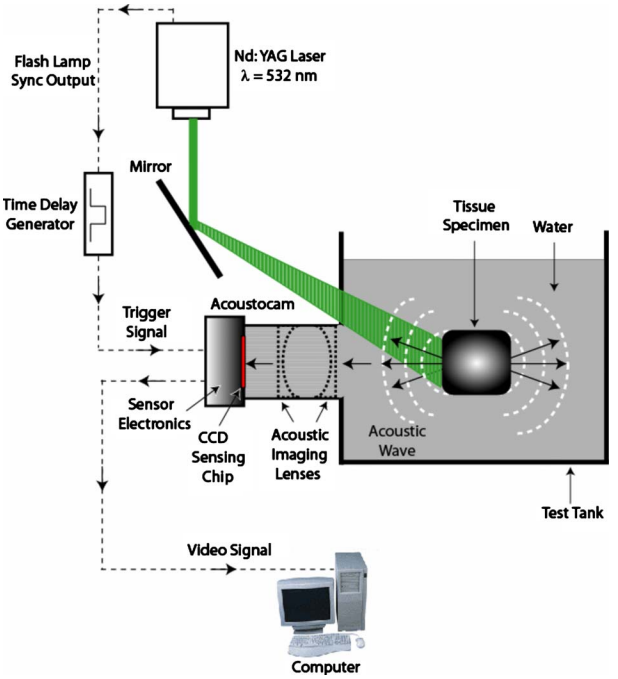

Fig. 1 A schematic diagram of the PA imaging system.

dimensional (2-D) transducer array system is a desirable alternative; however, they are significantly more expensive, and the reconstruction algorithms used for image formation can be time consuming. These may limit the application of PA imaging techniques in certain clinical environments where 2-D real-time imaging approaches are needed.

In this work, a novel PA imaging system that incorporates a commercial ultrasonic camera for real-time imaging of 2-D projection planes in tissue at video rate (30 Hz) is presented. The ultrasonic camera system offers several advantages compared with alternative techniques in PA imaging. Experimental results are reported for real-time PA imaging of optically absorbing targets in clear and turbid media, and the spatial resolution of the system is quantified.

2 Experimental Approach

The PA imaging system includes a pulsed laser for PA generation and an ultrasonic camera for imaging, as shown schematically in Fig. 1. The ultrasonic camera is referred to as the Acoustocam, which is manufactured by Imperium, Inc.,[15] and is commercially available.

2.1 *Ultrasonic Imaging Camera*

The Acoustocam is a real-time ultrasonic imaging camera that consists of a 2-D 12×12 mm charge-coupled device (CCD) chip, with 120×120 piezoelectric sensing elements used to sense the incoming ultrasonic pressure distribution from a PA source. An ultrasonic lens system is placed in front of the chip to collect the incoming PA signal and provides the ability for focusing and imaging at different depths. The focal depth of the lens system is 38 mm, and its f-number is 1. The chip and lens system are immersed in water that is encapsulated in a cylindrical tube. The electronic system that controls the imaging chip time-gates the detected ultrasonic signal according to

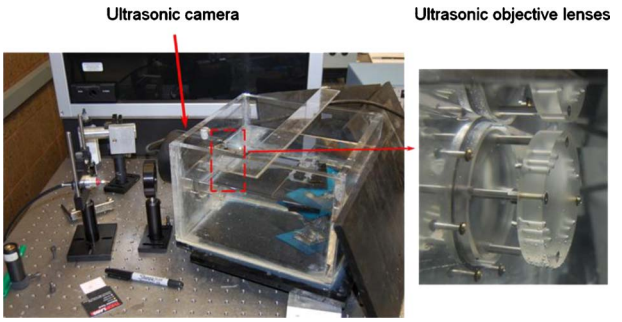

Fig. 2 A photograph of the PA imaging setup and the ultrasonic lens.

the time-of-arrival of the PA waves, selects the peak pressure at each pixel within the selected gate, and creates a real-time video of the PA source distribution, which can be monitored on a display or digitized in a computer for recording and processing. As a result, the imaging procedure mimics the maximum-amplitude-projection (MAP) operation used in PA microscopy[5] to produce a 2-D image along the projection plane that is parallel to the CCD surface.

The bandwidth of each transducer element is very broad, exceeding 10 MHz, and the CCD array has a frame rate of 30 Hz. The Acoustocam is widely used in nondestructive ultrasonic imaging of flaws and defects in engineering structures,[15–17] and with limited applications in ultrasonic imaging in biological media.[15,18] In such applications, a piezoelectric transducer is used to generate ultrasound, which is then used to insonify an object, and the scattered ultrasonic waves are imaged through the Acoustocam. In our work, laser-generated PA signals are directly imaged through the Acoustocam, and therefore an ultrasound generation transducer is not needed. The Acoustocam is an attractive alternative to expensive ultrasonic array transducers used for PA imaging because it is relatively inexpensive and compact. Furthermore, the use of an acoustic lens provides a long standoff distance from the test object, unlike a lensless array transducer system. The long standoff distance enables easier routing of the PA-generating laser beam to the tissue.

2.2 *Experimental Setup*

A photograph of the PA imaging system developed in this work is shown in Fig. 2. The generation laser (output wavelength: 532 nm; pulse width: 5 ns) irradiates the target specimen (PA source) placed in a water tank that is filled with deionized water. At the location of the target, the diameter of the laser beam is 25 mm, and the peak pulse energy of the laser is limited to 21 mJ, yielding an energy density of 4.28 $\mathrm{mJ/cm^2}$. The energy density is within the ANSI safety standard for the maximum permissible exposure of human skin to pulsed laser radiation in the visible spectral range.[19] The Acoustocam is mounted on one side of the water tank, as shown in Fig. 2. The operation of the Acoustocam is synchronized with the timing of the laser pulses emitted by the excitation source. This is achieved by triggering the Acoustocam with a transistor-transistor logic (TTL) output signal from a digital time delay generator, which is further triggered by the flashlamp synchronization output signal from the pulsed laser source. This arrangement allows for the adjustment of the

time delay between the flashlamp discharge and the laser output before triggering the Acoustocam for image acquisition.

The electronic time gate in the Acoustocam is used to control the time window during which the CCD chip is open for data acquisition. The front edge of the time gate is related to the travel time of the generated acoustic wave from the PA source to the plane of the CCD chip, while the rear gate is related to the duration of the PA pressure wave. It is worth noting that the choice of the Acoustocam time gate is critical since the camera creates an image based on the peak PA pressure at each pixel within the selected gate and does not retain time-resolved information.

3 Experimental Results and Discussion

3.1 *Spatial Resolution*

In the first set of experiments, the spatial resolution of the PA imaging system was evaluated by imaging an abrupt edge in an aluminum block with a milled slot of width 4.82 mm. The target specimen was placed in the water tank within the focal region of the ultrasonic camera lenses and illuminated with the generation laser. A piece of black tape was placed on the solid portion of the aluminum block to enhance the optical generation of pressure waves. The laser beam was expanded to illuminate a portion of the slot, and the 2-D PA image obtained with the ultrasonic camera is shown in Fig. 3(a) in gray scale. The pixel intensites in this figure, and all the following figures, are normalized to [0 1] with arbitrary unit. An electronic time gate of about 5 μs was applied to the PA signals received at each of the piezoelectric sensing elements of the acoustic camera. Within the selected time gate, the peak PA pressure wave amplitude was recorded and rendered in the image. The bright regions in the PA image result from optical generation of pressure waves on the black tape, and the dark region is the portion of the illuminated specimen where there is no optical generation. The peak pressure distribution across the dashed line in the acquired PA image is shown in Fig. 3(b). The lateral distance between the half points of the pressure peaks, which corresponds to the measured width of the slot, is approximately 5.0 mm. This value is in close agreement with the expected value of 4.8 mm.

The spatial resolution of the PA system was evaluated by measuring the line-spread-function of the measured abrupt edge. The analysis consists of processing the portion of the pressure wave data between 10 and 15 mm in Fig. 3(b). First, a spatial derivative of the data in Fig. 3(b) was taken, and the resulting line-spread-function obtained is shown in Fig. 3(c). The portion of Fig. 3(c) that pertains to the abrupt edge is highlighted in the figure.

In order to estimate the spatial resolution based on the line-spread-function, a spatial fast Fourier transform (FFT) of the highlighted portion of Fig. 3(c) was performed, resulting in the modulation transfer function shown in Fig. 3(d). The first zero crossing of the modulation transfer function occurs at 1.2 mm^{-1}, which provides an estimate of the maximum spatial frequency (ν_{max}) in the PA image. The reciprocal of ν_{max} yields the limiting spatial resolution of 0.78 mm.

A second calibration target [Fig. 4(a)] that was imaged consists of an aluminum block on which the letters *N* and *U* were milled out. The height of the letters is 15 mm, and the width is 10 mm. Black tape was pasted onto the block with

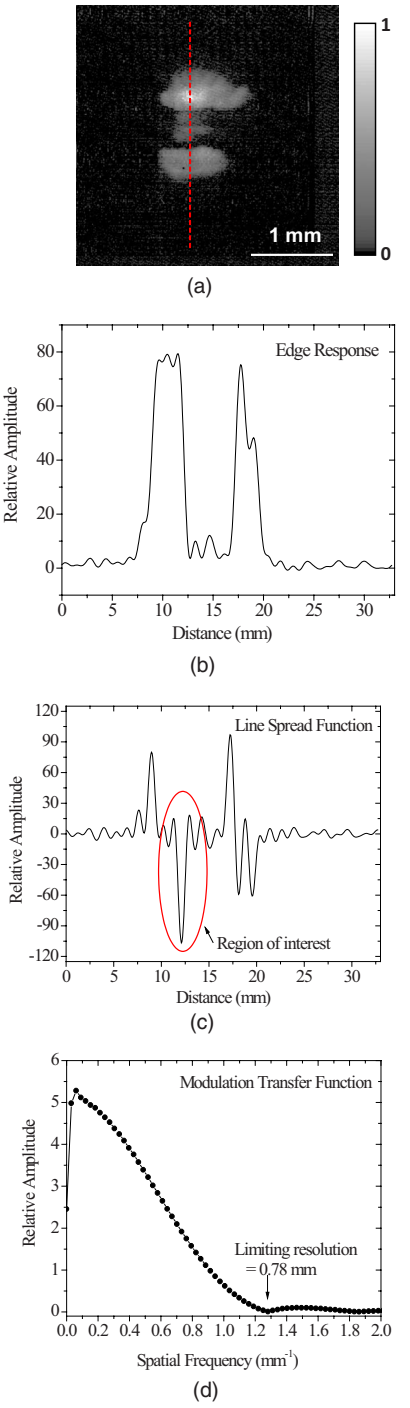

Fig. 3 PA imaging of a milled slot in an aluminum block. (a) 2-D projection of the PA image. (b) 1-D PA amplitude distribution along the highlighted line in (a). (c) First derivative of the PA amplitude distribution (b) along the abrupt edge. (d) Spatial Fourier transform of amplitude data in the highlighted region in (c).

the letters *N* and *U* cut out. When the target was illuminated by the laser beam, PA generation occurred only from the taped regions. The letters *N* and *U* are clearly visible [Figs. 4(b) and 4(c)] in this case, and the brighter circular regions represent the laser illuminated area. This demonstrates that the camera can image PA signals from large areas in a single shot. It is important to note that the letters *N* and *U* were separately

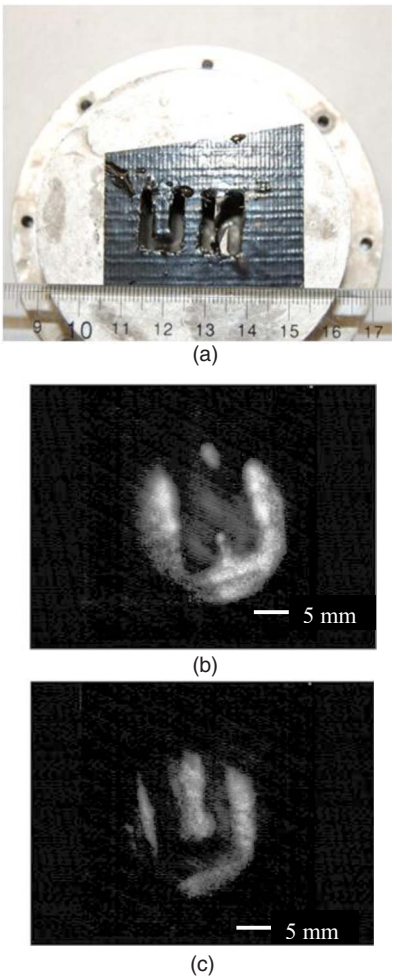

Fig. 4 PA imaging of a black-tape phantom in water. (a) Photograph of the specimen in which the letters *N* and *U* are milled out. (b) PA image showing the letter *N*. (c) PA image showing the letter *U*.

illuminated by the generation laser. The laser fluence was significantly reduced when the spot size of the generation laser was expanded to illuminate the features *N* and *U* simultaneously in the target specimen, leading to low PA pressure and poor signal-to-noise ratio.

3.2 *Real-Time Large-Area Imaging*

The real-time imaging capability of the PA imaging system was evaluated. In this case, two crossed graphite rods (diameter: 300 μm) were used as the target specimen [Fig. 5(a)]. The laser beam was scanned across the specimen, and the real-time image of the PA pressure wave radiating from the specimen was recorded at a frame rate of 30 Hz. A snapshot of the 2-D PA image is shown in Fig. 5(b), and a real-time video demonstrating the real-time capability of the system is available online (Video 1).

3.3 *Imaging in Tissue Samples*

PA imaging of an optically absorbing target through tissue specimens was also demonstrated. The first specimen used is a pair of rubber strings (diameter=1.68 mm) spaced 6 mm apart, imaged through 3-mm-thick chicken breast tissue. The

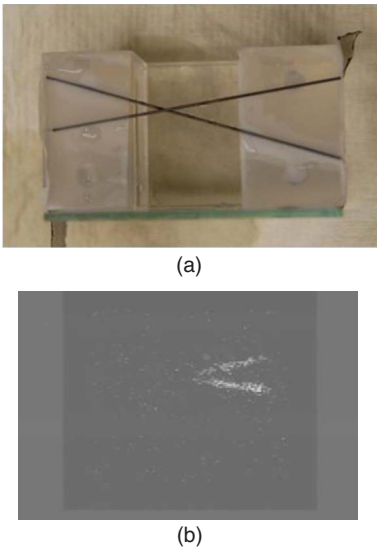

Fig. 5 PA imaging of graphite targets in water. (a) Photograph of a pair of crossed graphite rods. (b) PA image of a portion of the targets.

chicken breast tissue is optically turbid, which leads to scattering of the incident laser. Figure 6(a) shows the image of the rubber strings placed behind the tissue. The higher intensity regions in the image reveal the presence of the rubber strings behind the chicken tissue. Note that the strings were not parallel behind the tissue, as seen in the PA image. The pressure distribution along the dashed line in the image is shown in Fig. 6(b), where a lateral separation of approximately 5.5 mm between the strings is estimated. The strings are clearly resolved in the image; however, the FWHM of the first PA peak signal from the string is 900 μm, which is smaller than the expected value of 1.68 mm. This may be due to the reduction in the effective laser-irradiated region on the specimen surface due the effects of optical scattering.

The second tissue sample consisted of a piece of chicken breast tissue embedded with a single rubber string (diameter=1.68 mm) at a depth of approximately 4 mm below the tissue surface [Fig. 7(a)]. The embedded string strongly absorbs the light, and Fig. 7(b) shows the PA image obtained. The spatial extent of the rubber tube seen in the image is limited by the size of the excitation laser beam used,

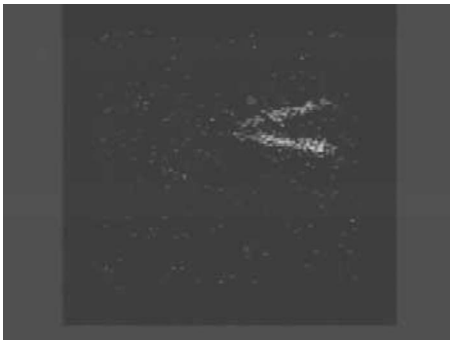

Video 1 Real-time video of PA imaging of a pair of crossed graphite rods taken as the illumination laser is scanned over the rods (MPEG, 7.3 MB). [URL: http://dx.doi.org/10.1117/1.3420079.1].

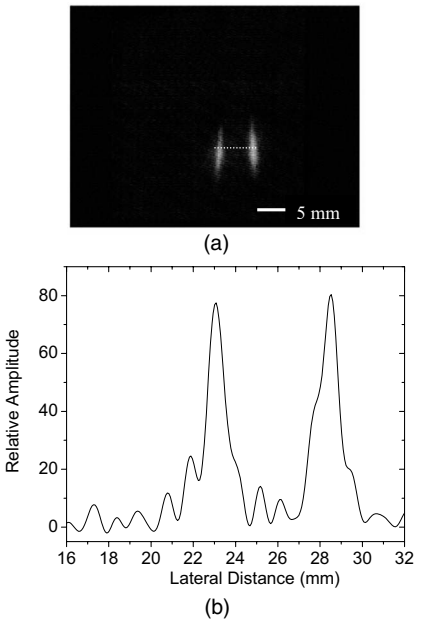

Fig. 6 PA imaging of rubber strings imaged through a slice of chicken breast tissue. (a) PA image. (b) The PA amplitude distribution along the highlighted line in (a).

which was approximately 10 mm. The generation laser spot size was reduced from the nominal value of 25 mm to 10 mm in order to increase the laser fluence. In this case, the optical fluence is 26.7 mJ/cm^2.

4 Conclusions

A real-time PA imaging system has been developed that is capable of rendering full-field 2-D projection images of the PA pressure wave distribution at video rate (30 Hz). The system incorporates a commercial ultrasonic camera, which houses a set of image forming lenses and 120×120 piezoelectric sensing elements. Images were acquired from samples in both optically clear and turbid media, while limiting the optical laser fluence to be within the ANSI limits for the maximum permissible exposure of human skin to pulsed laser radiation in the visible spectral range. The lateral spatial resolution of the system and its capability for real-time imaging were examined. Under the current operating conditions, the lateral spatial resolution of the system was estimated to be 0.78 mm. Compared with single-transducer-based PA imaging, our system can achieve a full-field projection imaging in real time based on a single laser pulse illumination. Compared with an ultrasonic array transducer–based PA imaging system, our system offers 2-D projection rather than cross-sectional imaging.

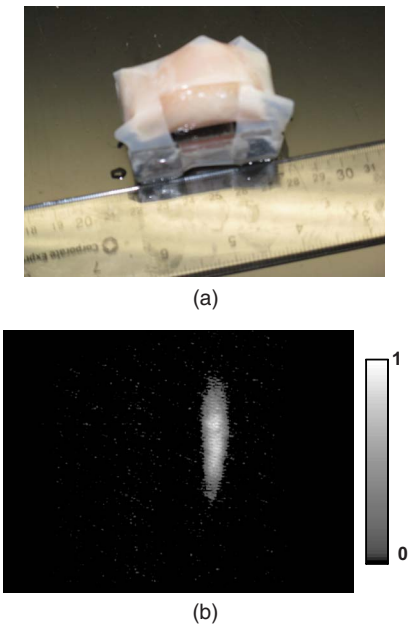

Fig. 7 PA imaging of a rubber string embedded in chicken breast tissue. (a) Photograph of the chicken specimen with the embedded string. (b) PA image of the rubber string.

Acknowledgments

The authors would like to thank David Rich and Bob Lasser from Imperium, Inc., for their prompt technical support. The authors also thank The Lynde and Harry Bradley Foundation and The Greater Milwaukee Foundation for their financial support to H. F. Zhang.

References

1. M. Xu and L. V. Wang, "Photoacoustic imaging in biomedicine," *Rev. Sci. Instrum.* **77**, 041101 (2006).
2. L. Wang, "Ultrasound-mediated biophotonic imaging: a review of acousto-optical tomography and photoacoustic tomography," *Dis. Markers* **15**, 123–138 (2003).
3. K. Maslov, H. F. Zhang, S. Hu, and L. V. Wang, "Optical-resolution photoacoustic microscopy for *in vivo* imaging of single capillaries," *Opt. Lett.* **33**, 929–931 (2008).
4. H. F. Zhang, K. Maslov, M.-L. Li, G. Stoica, and L. V. Wang, "*In vivo* volumetric imaging of subcutaneous microvasculature using photoacoustic microscopy," *Opt. Express* **14**, 9317–9323 (2006).
5. H. F. Zhang, K. Maslov, G. Stoica, and L. V. Wang, "Functional photoacoustic microscopy for high-resolution and noninvasive *in vivo* imaging," *Nat. Biotechnol.* **24**, 848–851 (2006).
6. R. Zemp, M. Li, R. Bitton, K. K. Shung, G. Stoica, and L. V. Wang, "Photoacoustic imaging of the microvasculature with a high-frequency ultrasound array transducer," *J. Biomed. Opt.* **12**, 010501 (2007).
7. J. J. Niederhauser, M. Jaeger, R. Lemor, P. Weber, and M. Frenz, "Combined ultrasound and optoacoustic system for real-time high contrast vascular imaging *in vivo*," *IEEE Trans. Med. Imaging* **24**, 436–440 (2005).
8. R. I. Siphanto, K. K. Thuma, T. G. Van Leewen, F. F. M. De Mul, J. W. Van Neck, L. N. Van Adrichem, and W. Steebergen, "Serial noninvasive photoacoustic imaging of neovascularization in tumor angiogenesis," *Opt. Express* **13**, 89–95 (2004).
9. R. O. Esenaliev, I. V. Larina, K. V. Larina, D. J. Deyo, M. Motamedi, and D. S. Prough, "Optoacoustic technique for noninvasive monitoring of blood oxygenation: a feasibility study," *Appl. Opt.* **43**, 3401 (2002).
10. Z. Zhao and R. Myllyla, "Photoacoustic determination of glucose concentration in whole blood by a near infrared laser diode," *Proc. SPIE* **4256**, 77–83 (2001).
11. K. Maslov, G. Stoica, and L. V. Wang, "*In vivo* dark field reflection mode photoacoustic microscopy," *Opt. Lett.* **30**, 625–627 (2005).
12. R. J. Zemp, L. Song, R. Bitton, K. K. Shung, and L. V. Wang, "Real-time photoacoustic microscopy *in vivo* with a 30-MHz ultrasound array transducer," *Opt. Express* **16**, 7915–7928 (2008).
13. S. Ermilov, A. Conjusteau, K. Mehta, R. Lacewell, P. M. Henrichs, and A. A. Oraevsky, "128 channel laser optoacoustic imaging system (LOIS-128) for breast cancer diagnostics," *Proc. SPIE* **6086**, 608609 (2006).

14. D. Yang, D. Xing, S. Yang, and L. Xiang, "Fast full-view photoacoustic imaging by combined scanning with a linear transducer array," *Opt. Express* **23**, 15566–15575 (2007).
15. Imperium, Inc., Silver Spring, MD; http://www.imperiuminc.com.
16. I. Komsky, S. Krishnaswamy, and B. Lasser, "Integration of different scanning modalities for real-time dual channel ultrasonic inspection of aircraft structures," in *Review of Progress in Quantitative Nondestructive Evaluation 27A and 27B*, *AIP Conf. Proc.* **975**, 1614–1621 (2008).
17. W. R. Davis and B. Lasser, "Real-time ultrasonic imaging using CCD camera techniques," in *Nondestructive Characterization of Materials XI*, pp. 135–140, Springer, New York (2003).
18. N. Parmar and M. C. Kolios, "An investigation of the use of transmission ultrasound to measure acoustic attenuation changes in thermal therapy," *Med. Biol. Eng. Comput.* **44**, 583–591 (2006).
19. American National Standards Institute, "American national standard for the safe use of lasers in health care facilities: standard Z136.1-2000," ANSI, Inc., New York (2000).